Cross-link Density Dependence of Spatial Inhomogeneities and Dynamic Fluctuations of Poly(*N*-isopropylacrylamide) Gels

Mitsuhiro Shibayama,* Tomohisa Norisuye, and Shunji Nomura

Department of Polymer Science and Engineering, Kyoto Institute of Technology, Matsugasaki, Sakyo-ku, Kyoto 606, Japan

Received July 11, 1996; Revised Manuscript Received October 25, 1996[⊗]

ABSTRACT: Dynamic light scattering studies have been carried out on poly(*N*-isopropylacrylamide) (NIPA) gels having different cross-link densities. Intensity−intensity time correlation functions obtained at 25 °C were successfully analyzed by taking account of the nonergodic nature of gels. By taking the ensemble average ($\langle I \rangle_E$) of the time average scattered intensity ($\langle I \rangle_T$), the dynamic component of the concentration fluctuations ($\langle I_F \rangle_T$) and the spatial inhomogeneities ($\langle I \rangle_E$; the ensemble average) were evaluated as a function of cross-link density. While $\langle I_F \rangle_T$ remained more or less constant, $\langle I \rangle_E$ increased with the increasing ratio of cross-linker concentration (C_{BIS}) to the monomer concentration (C_{NIPA}), $r \equiv C_{BIS}/C_{NIPA}$, where BIS is the abbreviation of the cross-linker, *N*,*N*′-methylenebis(acrylamide). This indicates domination of the static inhomogeneity for large *r*. The correlation length, ξ, a measure of the range of dynamic fluctuations, was evaluated from the time correlation function. A linear relationship was obtained for ξ^{-1}, i.e., $1/\xi = (1/\xi_{soln}) + (1/\xi_{gel})r$, with $\xi_{soln} = 144$ Å and $\xi_{gel} = 8.12$ Å. The value of ξ_{gel} was found to be in good agreement with the literature value for the segment length of NIPA polymers, 8.12 Å.

Introduction

When we observe a gel under a microscope with an irradiation of a laser beam, we notice the presence of fluctuating speckles along the beam passing through the gel.[1] In the case of polymer solutions, speckles are not usually observed while bright tiny spots are moving along the local flow of the solution. This is called the Tyndall phenomenon. On the other hand, glassy plastics exhibit nonfluctuating speckles due to surface roughness and/or refractive index fluctuations in it.[2] This example indicates that a gel is an intermediate material between glassy materials and liquids. Pusey and van Megen noticed this type of fluctuations and proposed a theory to deal with viscous fluid.[3] This is a theory for dynamic light scattering (DLS) on the basis of the concept of nonergodicity. In the case of glasses and gels, the scattering elements are able only to make limited Brownian excursions about the fixed average positions. This is the origin of the time-fluctuating speckles. For such systems, we have to distinguish strictly the time and ensemble averages.

Gels are topologically frozen structures. In other words, the ensemble of observation is different from that of preparation in the case of gels.[4] This leads to a breakdown of the assumption of ergodicity. From static scattering experiments, it is now clear that the concentration fluctuations of gels comprise both static inhomogeneities (frozen structure) and dynamic fluctuations.[5−11] This statement is symbolized by the following equation:

$$I(q) \equiv \langle I(q) \rangle_T = I_C(q) + \langle I_F(q) \rangle_T \quad (1)$$

where $I(q)$ is the total scattered intensity, q is the magnitude of the scattering vector, and $I_C(q)$ and $I_F(q)$ are the scattered intensity due to the frozen structure and liquidlike concentration fluctuations, respectively, and $\langle ... \rangle_T$ denotes time average. As a matter of fact, $I_C(q)$ is a position dependent quantity because of the presence of spatial inhomonegeity. Since scattering elements in a gel are allowed only a limited excursion in the phase space because of the topological constraint, $I(q)$ is position (p) dependent and an ensemble average has to be taken, i.e.,

$$I(q) \equiv \langle I(q) \rangle_E = \lim_{P \to \infty} \frac{1}{P} \sum_{p=1}^{P} \{I_{C,p}(q) + I_F(q)\} = \langle I_C(q,t) \rangle_E + \langle I_F(q,t) \rangle_E \quad (2)$$

where $\langle ... \rangle_E$ denotes ensemble average. Note that $\langle I_F(q,t) \rangle_E = \langle I_F(q,t) \rangle_T$. The concept of nonergodicity of gels, first pointed out by Pusey and van Megen,[3] has led to the development of several relevant methods to analyze the dynamic properties of gels, such as the nonergodic medium method by Pusey and van Megen and the heterodyne method by Joosten et al.[12,13] The validity of these analyses were examined by Fang and Brown.[14]

In a previous paper, we dealt with copolymer gels consisting of poly(*N*-isopropylacrylamide-*co*-acrylic acid) (NIPA/AAc) and discussed the comonomer concentration and temperature dependence of the dynamic fluctuations and the static inhomogeneities.[15] Divergence of both ensemble and time average scattered intensities at the critical temperature was observed. This is due to strong temperature dependence of the solubility of NIPA polymers in water. In this paper, we discuss the origin of cross-link inhomogeneities on polymer gels by DLS. Both preparation and observation temperatures were kept low enough to avoid effects of critical opalescence. Thus, we assume that the concentration fluctuations are solely due to thermal (dynamic) fluctuations and cross-link (frozen) inhomogeneities. Scattered intensity was measured at different sample positions and the ensemble average scattered intensity was obtained as a function of cross-link density, from which structural parameters were evaluated. A simple relationship between the cross-link density and these parameters will be proposed.

Experimental Section

NIPA polymer solutions and gels were prepared by conventional redox polymerization. Prescribed amounts of NIPA (690

* To whom correspondence should be addressed.

[⊗] Abstract published in *Advance ACS Abstracts,* December 15, 1996.

S0024-9297(96)00999-0 CCC: $12.00

Table 1. Sample Code and Concentrations

code	C_{NIPA} (mM)	C_{BIS} (mM)	$r = C_{BIS}/C_{NIPA}$ ($\times 10^2$)
NB000	690	0	0
NB063	690	4.31	0.63
NB125	690	8.62	1.25
NB187	690	12.9	1.87
NB223	690	15.4	2.23
NB259	690	17.9	2.59
NB293	690	20.2	2.93
NB325	690	22.4	3.25

mM), *N*,*N*′-methylenebis(acrylamide) (BIS) (for the gels only), and ammonium persulfate (APS) (8 mM) were dissolved in deionized water. The numbers in the parentheses indicate the concentrations in the pregel solution. After complete dissolution, the solution was degassed and stored in a refrigerator to suppress the polymerization reaction. Polymerization was initiated in a 10 mm diameter test tube by adding 1.75 mM of *N*,*N*,*N*′,*N*′-tetramethylethylenediamine (TEMED) at 20 °C. The monomer, C_{NIPA}, and cross-linker concentrations, C_{BIS}, as well as the ratio of these, $r \equiv C_{BIS}/C_{NIPA}$, are listed in Table 1.

Dynamic light scattering (DLS) experiments were carried out on a laboratory made optics apparatus equipped with a 5 mW He−Ne laser. The scattering angle was fixed to be 60°. Photon correlation was taken with a DLS-7 photon correlator, Otsuka Electric Co. All measurements were made on reactor batch samples at 25 °C.

Results and Discussion

Though experiments and analyses were conducted on all the samples listed in Table 1, we show results on only for NB000, NB223, and NB325 in most of the following figures.

Figure 1 shows intensity fluctuations with sample positions for (a) NIPA polymer solution (NB000) and NIPA gels with different cross-link densities; (b) r = 0.0223 (NB223) and (c) 0.0325 (NB325). In the case of the NIPA solution (r = 0), fluctuations of the time average scattered intensity, $\langle I\rangle_T$, are relatively small. Note that $\langle I\rangle_T$ is simply obtained by measuring scattered intensity at a single position (and at a given angle). The ensemble average scattered intensity, $\langle I\rangle_E$, is obtained by averaging $\langle I\rangle_T$ (obtained at different sample positions), which is depicted by the dotted line. The identity $\langle I\rangle_E = \langle I\rangle_T = \langle I_F\rangle_T$ is expected, because a polymer solution is an ergodic medium. However, a deviation of $\langle I\rangle_E$ from $\langle I_F\rangle_T$ is already seen in NB000, which is explained as follows: Even in NIPA polymer solutions, temporal cross-links are formed via hydrophobic association of *N*-isopropyl groups, which lead to a gellike behavior. As a matter of fact, the NIPA polymer solution hardly flowed even by turning the test tube upside down and it showed a viscoelastic behavior. The formation of temporal cross-links is also speculated by the observation of a deviation of Ornstein−Zernike function type behavior in the static structure factor examined by small-angle neutron scattering.[9,16] This kind of nonergodicity was not observed in polymer solutions without a hydrophobic moiety. By introducing cross-links, strong fluctuations in $\langle I\rangle_T$ appear. The time average intensity, $\langle I\rangle_T$, highly fluctuates with sample position by increasing r. Accordingly, $\langle I\rangle_E$ increases. Note that the plot of $\langle I\rangle_T$ for NB325 is truncated so as to compare $\langle I\rangle_E$'s in the same scale. The dashed line indicates the time fluctuating component of the scattered intensity, $\langle I_F\rangle_T$, whose evaluation will be discussed in conjunction with Figures 3 and 4.

An intensity−intensity time correlation function, $g^{(2)}(\tau)$, was obtained for each sample position of each sample. $g^{(2)}(\tau)$ is given by[3,13,17,18]

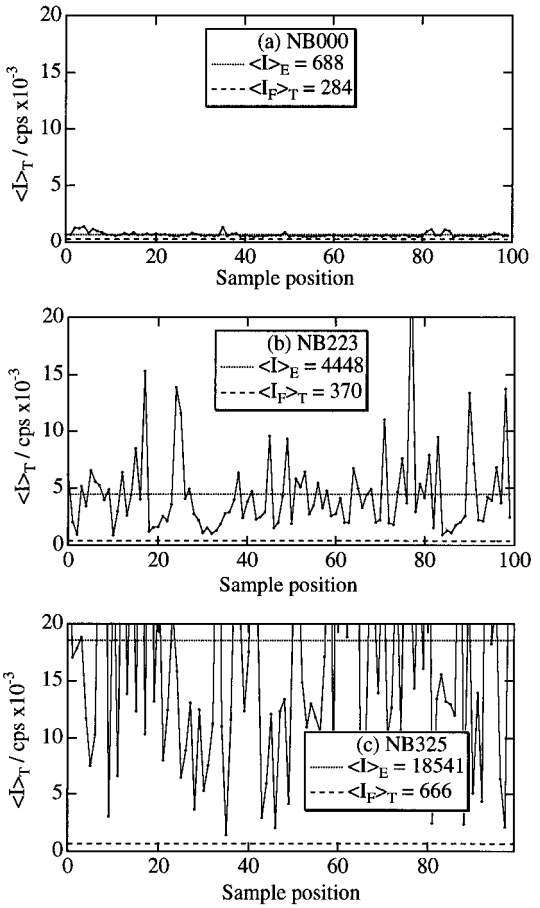

Figure 1. Time average scattered intensity, $\langle I\rangle_T$, vs sample position for (a) NIPA polymer solution (NB000) and NIPA gels (b) NB223 and (c) NB325. The dotted and dashed lines indicate the ensemble average scattered intensity, $\langle I\rangle_E$, and the time-fluctuating component of the scattered intensity, $\langle I_F\rangle_T$.

$$g^{(2)}(\tau) = \beta\sigma_I^{\,2} \exp[-2D_A q^2\tau] + 1 = \sigma_{I,obs}^{\,2} \exp[-2D_A q^2\tau] + 1 \quad (3)$$

where D_A is the apparent diffusion coefficient, and β ($\equiv\sigma_{I,obs}^2/\sigma_I^2$) is the instrumental coherence factor ($0 < \beta < 1$). σ_I^2 denotes the initial amplitude of $g^{(2)}(\tau)$ and $\sigma_{I,obs}^2$ is that at observation. Figure 2 shows a typical intensity−intensity time correlation function, $g^{(2)}(\tau)$, for (a) NB125 and (b) NB325. The solid curves indicate fitted curves with eq 3, from which the apparent diffusion coefficient D_A's were estimated. These figures indicate that a single exponential fit is satisfactory for polymer gels, which is due to cooperativity of gel dynamics.[18] It should be noted here that $g^{(2)}(0)$ is far below 2, indicating nonergodic nature of gels.

According to Joosten et al., the diffusion coefficient of nonergodic medium, D, can be evaluated by plotting D_A as a function of $\langle I\rangle_T$, owing to the following relationship:[13]

$$D = \frac{D_A}{2 - X} = \frac{D_A}{2 - \langle I_F\rangle_T/\langle I\rangle_T} \quad (4)$$

where X is given by

$$X \equiv \frac{\langle I_F(q)\rangle_T}{\langle I(q)\rangle_T} \quad (5)$$

Note that the cases of $X = 1$ ($D_A = D$) and $X = 0$ ($D_A =$

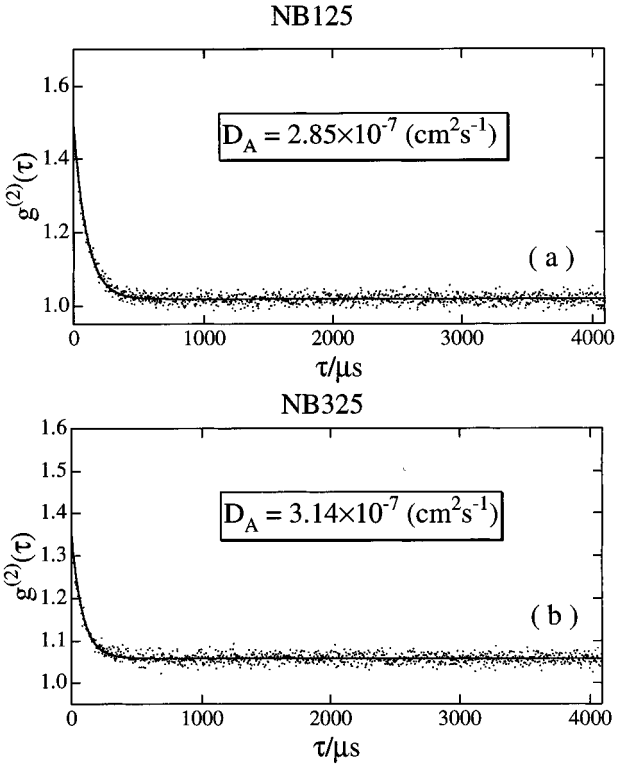

Figure 2. Intensity−intensity time correlation function, $g^{(2)}(\tau)$, for (a) NB125 and (b) NB325. D_A is the apparent diffusion coefficient estimated with eq 3.

$2D$) correspond a pure homodyne mode and pure heterodyne mode, respectively. For the nonergodic medium, a partial heterodyne mode is given at $0 < X < 1$. Figure 3 shows the variation of the apparent diffusion constant, D_A, with time average scattered intensity, $\langle I\rangle_T$, for (a) NB000, (b) NB223, and (c) NB325. Note that D_A for polymer solutions is also dependent on $\langle I\rangle_T$. This indicates that the NIPA solution also has a nonergodic nature to some extent, as discussed above. In the case of gels, D_A's are mapped nicely onto a convex function (solid curves in the figures), as predicted by eq 4, from which the cooperative diffusion coefficient, D, $\langle I_F\rangle_T$, and the initial amplitude, $\sigma_{I,obs}{}^2$, are evaluated.

However, it may be more convenient to rewrite eq 4 in the following form for analyzing experimental data:[15]

$$\frac{\langle I\rangle_T}{D_A} = \frac{2}{D}\langle I\rangle_T - \frac{\langle I_F\rangle_T}{D} \tag{6}$$

Figure 4 shows the plot of $\langle I\rangle_T/D_A$ vs $\langle I\rangle_T$ for (a) NB000, (b) NB223, and (c) NB325. As shown in the figure, the data points are nicely collapsed on a straight line, indicating the validity of the heterodyne mode analysis. It should be noted here that the linear regression analysis with eq 6 has to be conducted with a weighting function of the form of $1/\langle I\rangle_T$ so as to obtain the same results with those by eq 4. Otherwise this analysis will lead to an over- or underestimation of $\langle I_F\rangle_T$ because the range of $\langle I\rangle_T$ is very wide and the intercept $\langle I_F\rangle_T/D$ is very close to the origin. By taking account of this fact, D and $\langle I_F\rangle_T$ were evaluated from the slope and intercept.

Figure 5 shows the variation of (a) $\langle I\rangle_E$ as well as (b) $\langle I_F\rangle_T$ as a function of r. The increase in $\langle I\rangle_E$ with r is due to domination of static (frozen-in) inhomogeneities by increasing the cross-link density. Though the r

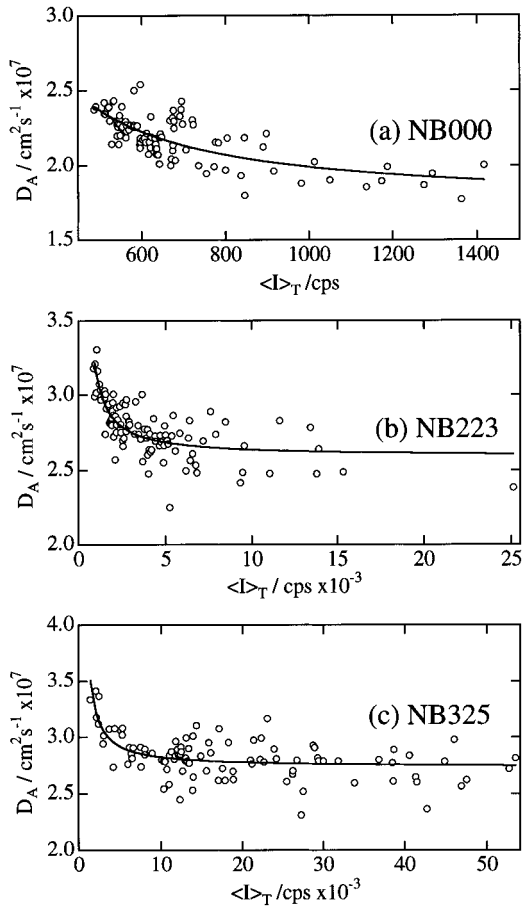

Figure 3. Apparent diffusion coefficient, D_A, vs time average scattered intensity, $\langle I\rangle_T$, for (a) NB000, (b) NB223, and (c) NB325.

dependence looks like a diverging function at around $r \approx 3 \times 10^{-2}$, no definitive functional form was resolved at this stage. On the other hand, $\langle I_F\rangle_T$ does not seem to be strongly dependent on r and is constant in this range, as indicated with the dashed line. One plausible explanation is given as follows: Because $\langle I_F\rangle_T$ is the time-fluctuating component of the scattered intensity, which is an excess scattering above the static scattering from frozen structure, it does not depend on cross-link density but on temperature. We will discuss this issue in conjunction with Figure 7. It should be noted that in the case of temperature dependence, a steep rise of $\langle I_F\rangle_T$ was observed both NIPA gels as well as NIPA-*co*-acrylic acid copolymer gels.[15]

Figure 6 shows D as a function of r. D seems to be a linear function of r, and D increases with r. This is accounted for by decreasing the correlation length ξ by increasing the cross-link density. The correlation length ξ is related to the diffusion coefficient D by the analogy of the Stokes−Einstein relationship as follows[4]

$$D \cong \frac{kT}{6\pi\eta\xi} \tag{7}$$

where η is the solvent viscosity (0.892×10^{-3} (N·s)/m^2; water at 25 °C) and kT is the Boltzmann energy. The inverse of ξ is also plotted as a function of r in Figure 6 by using the right ordinate. The linear relationship of D with r indicates an additivity of inverse ξ.

$$\frac{1}{\xi} = \frac{1}{\xi_{soln}} + \frac{1}{\xi_{gel}}r \tag{8}$$

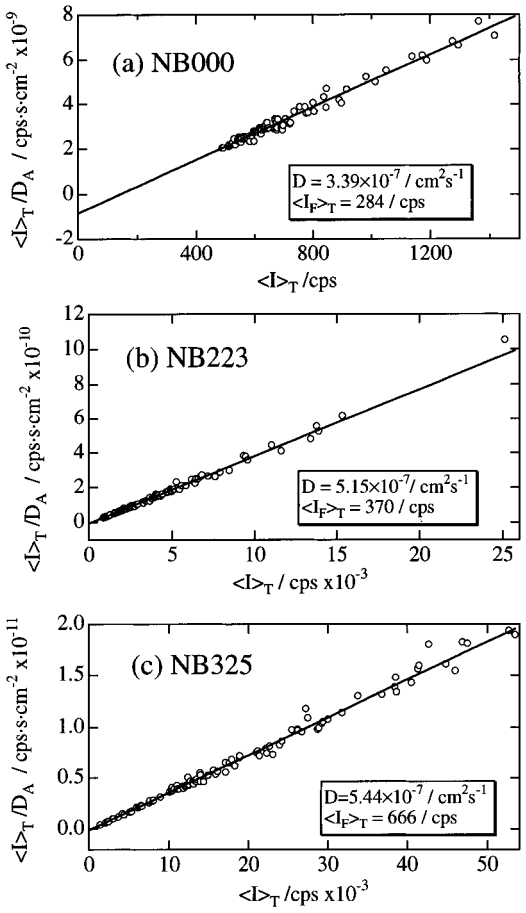

Figure 4. $\langle I\rangle_T/D_A$ vs $\langle I\rangle_T$ plot for (a) NB000, (b) NB223, and (c) NB325. The straight lines indicate fits with eq 6.

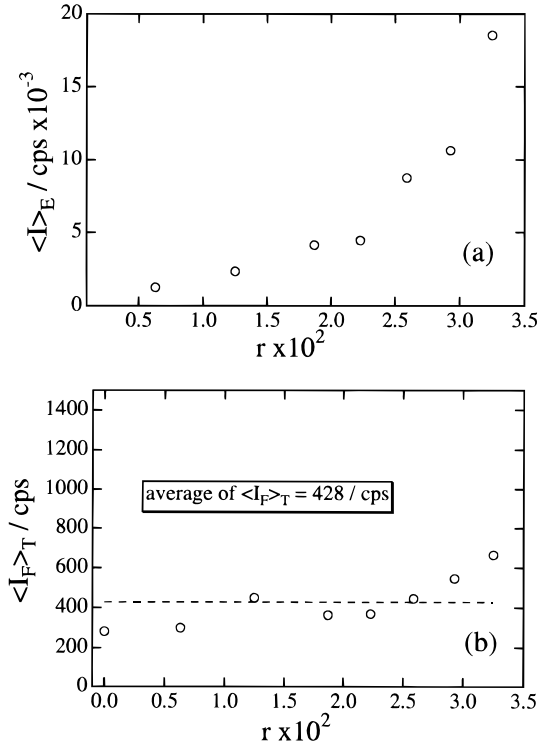

Figure 5. (a) Cross-link density, *r*, dependence of ensemble average scattered intensity, $\langle I\rangle_E$, and (b) dynamic component of time average scattered intensity, $\langle I_F\rangle_T$. The dashed line indicates the average of $\langle I_F\rangle_T$.

where ξ_{soln} and ξ_{gel} are the correlation length for a polymer solution and that for the limit of highly cross-linked network. As shown in the figure, the data points fit a straight line. The intercept of $r = 0$ gives ξ_{soln}^{-1}, and the slope gives ξ_{gel}^{-1}, respectively. The evaluated values are $\xi_{soln} = 144$ Å and $\xi_{gel} = 8.12$ Å. The latter is in good agreement with the literature value for the segment length of NIPA polymers, 8.12 Å.[19] No theory to account for the additivity of ξ^{-1} with respect to *r* has been proposed so far. This observed relation, however, suggests that an addition of cross-links results in lowering of ξ in this fashion although eq 8 is verified only in a very limited region of r ($0 \le r \le 0.0325$). It is interesting to compare the cross-linker effect (eq 8) with the polymer concentration effect, i.e., $\xi \sim \phi^{-3/4}$ for semidilute polymer solutions, where ϕ is the volume fraction of the polymer.

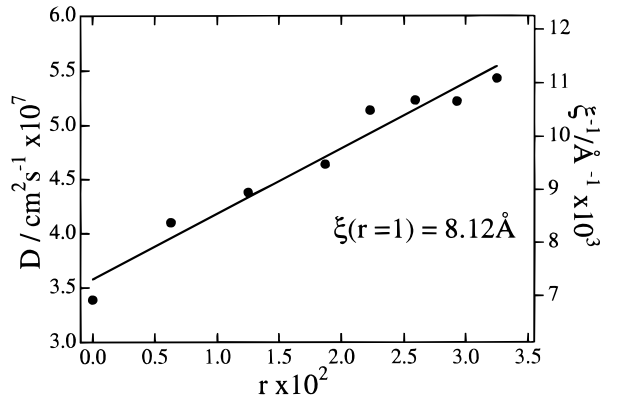

Figure 6. Cross-link density, *r*, dependence of diffusion coefficient, *D* (left), and inverse correlation length, ξ^{-1} (right).

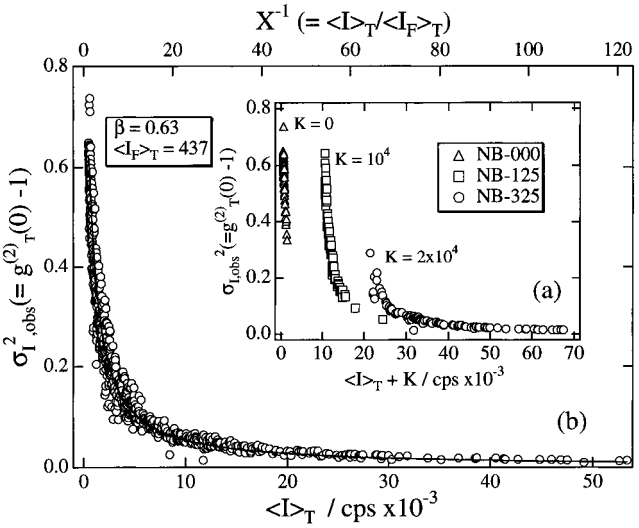

Figure 7. (a) Observed initial amplitude of the correlation function, $\sigma_{I,obs}^2$, vs $\langle I\rangle_T$ plots for (a) NB000, (b) NB223, and (c) NB325. *K* is the offset for the horizontal shift. (b) Master curve of $\sigma_{I,obs}^2$ as a function of $\langle I\rangle_T$ for all samples.

Figure 7a shows the initial amplitude of the correlation function, $\sigma_{I,obs}^2$, as a function of $\langle I\rangle_T$ for (a) NB000, (b) NB223, and (c) NB325. Note that the horizontal offset, *K*, is applied for NB223 and NB325. The higher the cross-link density, the higher $\langle I\rangle_T$ is, indicating a heterodyne mode becomes dominant. The values of $\sigma_{I,obs}^2$ are highly scattered with $\langle I\rangle_T$, but fall on a single curve, indicating that $\sigma_{I,obs}^2$ is a function of $\langle I\rangle_T$, i.e.,[13]

$$\sigma_{I,obs}{}^2 \equiv \beta\sigma_I{}^2 = \beta\left\{1 - \left(\frac{\langle I_F(q)\rangle_T}{\langle I(q)\rangle_T} - 1\right)^2\right\} \qquad (9)$$

The *r* dependence of $\sigma_{I,obs}^2$ is clear. The lower *r*, the

higher $\sigma_{I,obs}^2$ is. The physical meaning of $\sigma_{I,obs}^2$ becomes more distinct by plotting $\sigma_{I,obs}^2$ of all samples together. Figure 7b shows a master curve of $\sigma_{I,obs}^2$ as a function of $\langle I \rangle_T$. Surprisingly, all of the data points, i.e., 800 data points, taken from gels having different cross-link densities, are collapsed on a single master curve. The functional form of the master curve is given by eq 9. However, it should be noted that if $\langle I_F \rangle_T$ is different from sample to sample with different r's, such a superposition rule does not hold, as is obvious in eq 9. Therefore, this superposition indicates that $\langle I_F \rangle_T$ is more or less constant for all the samples studied here. This further indicates that $\langle I_F \rangle_T$ is independent of the cross-linker concentration and reflects solely the dynamic fluctuations of the system. Thus, the static inhomogeneities are extracted in I_C, i.e.,

$$I_C(p) = I(p) - \langle I_F \rangle_T \tag{10}$$

or

$$\langle I_C(p) \rangle_E = \langle I(p) - \langle I_F \rangle_T \rangle_E = \langle I \rangle_E - \langle I_F \rangle_T \tag{11}$$

This means that the separation of the dynamic fluctuations and static inhomogeneities can be conducted by this method.

Another important outcome of this analysis is the evaluation of the instrumental coherence factor β. In our system, β was estimated to be 0.63 by this analysis.[20] This master relationship of $\sigma_{I,obs}^2$ strongly indicates that the position dependent thermal fluctuations of gels can be characterized by a single parameter, $\langle I_F \rangle_T$ or $\langle I_F \rangle_T / \langle I \rangle_T$, irrespective of cross-link density. However, the shape of the master curve probably changes with temperature since $\langle I_F \rangle_T$ is a function of temperature. The validity of the last statement is now being examined.

Concluding Remarks

Static and dynamic properties of *N*-isopropylacrylamide gels were successfully analyzed by employing the heterodyne method. Fluctuations in $\langle I \rangle_T$ become larger with increasing the cross-linker to the monomer concentration ratio, r. This corresponds to an increase of $\langle I \rangle_E$. The cooperative diffusion coefficient, D, and the time-fluctuating scattered intensity, $\langle I_F \rangle_T$, were extracted by plotting $\langle I \rangle_T / D_A$ vs $\langle I \rangle_T$, where D_A is the apparent diffusion coefficient. D is a linear increasing function of r, which led to an additive relationship of the inverse of correlation length, ξ^{-1}, i.e., $1/\xi = 1/\xi_{soln} + r/\xi_{gel}$. The values of ξ_{soln} and ξ_{gel} were estimated to be 144 and 8.12 Å, respectively. The latter is in good agreement with the segment length of the NIPA monomer (8.12 Å), the limiting value of mesh size. A master curve was obtained for $\sigma_{I,obs}^2$ for all samples including the polymer solution. This indicates that σ_I^2 does not depend on r but on $\langle I \rangle_T$. A similar property was also obtained for $\langle I_F \rangle_T$. These findings indicate that the position dependent thermal fluctuations of gels can be characterized by a single parameter, $\langle I_F \rangle_T$ or $\langle I_F \rangle_T / \langle I \rangle_T$, irrespective of cross-link density. The master curve analysis allows one to evaluate the instrumental coherence factor, β, which is 0.63 in our particular case.

Acknowledgment. This work is supported by the Ministry of Education, Science, Sports, and Culture, Japan (Grant-in-Aid, No. 07241242 and 08231245 to M.S.).

References and Notes

(1) Orkisz, M. J. P. Ph.D. dissertation, Physics Department, Massachusetts Institute of Technology, 1994.
(2) Dainty, J. C., Ed. *Laser Speckle and Related Phenomena*; Springer-Verlag: Berlin, 1975.
(3) Pusey, P. N.; van Megen, W. *Physica A* **1989**, *157*, 705.
(4) de Gennes, P. G. *Scaling Concepts in Polymer Physics*; Cornell University Press: Ithaca, NY, 1979.
(5) Hecht, A. M.; Duplessix, R.; Geissler, E. *Macromolecules* **1985**, *18*, 2167.
(6) Mallam, S.; Horkay, F.; Hecht, A. M.; Geissler, E. *Macromolecules* **1991**, *24*, 543.
(7) Horkay, F.; Hecht, A. M.; Mallam, S.; Geissler, E.; Renie, A. R. *Macromolecules* **1991**, *24*, 2896.
(8) Cohen, Y.; Ramon, O.; Kopelman, I. J.; Mizrahi, S. *J. Polym. Sci., Polym. Phys. Ed.* **1992**, *30*, 1055.
(9) Shibayama, M.; Tanaka, T.; Han, C. C. *J. Chem. Phys.* **1992**, *97*, 6829.
(10) Rouf, C.; Bastide, J.; Pujol, J. M.; Schosseler, F.; Munch, J. P. *Phys. Rev. Lett.* **1994**, *73*, 830.
(11) Bastide, J.; Candau, S. J. In *Physical Properties of Gels*; Cohen Addad, J. P. Ed.; John Wiley & Sons: New York, 1996.
(12) Joosten, J. G. H.; Gelade, E.; Pusey, P. N. *Phys. Rev. A* **1990**, *42*, 2161.
(13) Joosten, J. G. H.; McCarthy, J. L.; Pusey, P. N. *Macromolecules* **1991**, *24*, 6690.
(14) Fang, L.; Brown, W. *Macromolecules* **1992**, *25*, 6897.
(15) Shibayama, M.; Fujikawa, Y.; Nomura, S. *Macromolecules* **1996**, *29*, 6535.
(16) Shibayama, M.; Tanaka, T. *J. Chem. Phys.* **1995**, *102*, 9392.
(17) Shibayama, M.; Takeuchi, T.; Nomura, S. *Macromolecules* **1994**, *27*, 5390.
(18) Tanaka, T.; Hocker, L. O.; Benedek, G. B. *J. Chem. Phys.* **1973**, *59*, 5151.
(19) Kubota, K.; Fujishige, S.; Ando, I. *Polym. J.* **1990**, *22*, 15.
(20) The instrumental coherence factor, β, estimated here is somewhat smaller than the value obtained by a standard sample, e.g., polystyrene latex. In the case of the latter, we obtained $\beta \geq 0.8$. The reason for this discrepancy is not clear at this stage.

MA9609994